

Quantum Chaos Diagnostics for Open Quantum Systems from Bi-Lanczos Krylov Dynamics

Matteo Baggioli,^{1,2,3} Kyoung-Bum Huh,² Hyun-Sik Jeong,^{4,5,6}
Xuhao Jiang,^{2,7,8} Keun-Young Kim^{9,10} and Juan F. Pedraza⁴

¹*School of Physics and Astronomy, Shanghai Jiao Tong University, Shanghai 200240, China*

²*Wilczek Quantum Center, School of Physics and Astronomy,
Shanghai Jiao Tong University, Shanghai 200240, China*

³*Shanghai Research Center for Quantum Sciences, Shanghai 201315, China*

⁴*Instituto de Física Teórica UAM/CSIC, Calle Nicolás Cabrera 13-15, 28049 Madrid, Spain*

⁵*Asia Pacific Center for Theoretical Physics, Pohang 37673, Korea*

⁶*Department of Physics, Pohang University of Science and Technology, Pohang 37673, Korea*

⁷*Technical University of Munich, TUM School of Natural Sciences, Physics Department, 85748 Garching, Germany*

⁸*Faculty for Physik, Ludwig-Maximilians-Universität München, Schellingstraße 4, 80799, Munich, Germany*

⁹*Department of Physics and Photon Science, Gwangju Institute of Science and Technology, Gwangju 61005, Korea and*

¹⁰*Research Center for Photon Science Technology,
Gwangju Institute of Science and Technology, Gwangju 61005, Korea*

In Hermitian systems, Krylov complexity has emerged as a powerful diagnostic of quantum dynamics, capable of distinguishing chaotic from integrable phases, in agreement with established probes such as spectral statistics and out-of-time-order correlators. By contrast, its role in non-Hermitian settings, relevant for modeling open quantum systems, remains less understood due to the challenges posed by complex eigenvalues and the limitations of standard approaches such as singular value decomposition. Here, we demonstrate that Krylov complexity, computed via the bi-Lanczos algorithm, effectively identifies chaotic and integrable phases in open quantum systems. The results align with complex spectral statistics and complex spacing ratios, highlighting the robustness of this approach. The universality of our findings is further supported through studies of both the non-Hermitian Sachdev-Ye-Kitaev model and non-Hermitian random matrix ensembles.

Introduction. The search for universal diagnostics of quantum chaos remains a central pursuit in the study of many-body quantum systems. Among the emerging approaches, Krylov complexity (KC) [1–3] has recently gained prominence as a sensitive probe of quantum dynamics. For recent comprehensive overviews, see [4, 5].

KC quantifies how rapidly an operator or state explores the Krylov subspace generated by time evolution, thereby encoding the dynamical growth of complexity. In closed (Hermitian) systems, particularly in the state-based formulation, where KC is entirely determined by the energy spectrum, it has been shown to reliably distinguish chaotic from integrable phases, in agreement with traditional spectral diagnostics such as level spacing statistics and spectral form factors [6–11].

However, realistic quantum systems are often coupled to their environment, leading to non-Hermitian effective dynamics that behave fundamentally differently from their closed counterparts [12, 13]. In such open systems, spectral analysis reveals universal signatures through complex eigenvalue statistics [14, 15]: integrable systems exhibit a two-dimensional Poisson distribution, while chaotic ones follow a Ginibre distribution [16].

The universal emergence of Ginibre statistics in non-Hermitian many-body systems [17–22] supports the Grobe-Haake-Sommers conjecture [14], namely the non-Hermitian counterpart to the Berry-Tabor and Bohigas-Giannoni-Schmit conjectures [23, 24] in the context of random matrix theory (RMT) [25]. In particular, Gini-

bre statistics define class A of non-Hermitian RMT [26]. A complementary probe is the complex spacing ratio (CSR) [19], a generalization of the r -parameter [27] to complex spectra, which identifies chaos through cubic radial repulsion and angular anisotropy.

Given the success of state-based Krylov complexity in diagnosing quantum chaos in closed systems, a natural question arises: *Can KC remain a reliable chaos indicator in open, non-Hermitian settings?* Despite growing interest in non-Hermitian dynamics, KC has not yet been systematically explored in this context. Naive extensions, such as those based on singular value decomposition [28, 29], face critical challenges due to the inherent complexity of non-Hermitian evolution and the biorthogonal nature of eigenstates, and thus fail to reliably discriminate between quantum chaos and integrability [30].

In this work, we address this gap by formulating a biorthogonal Krylov recursion via the bi-Lanczos algorithm, which naturally accounts for the non-Hermitian character of open systems. We demonstrate that KC reliably distinguishes chaotic from integrable dynamics in open quantum systems, in agreement with complex spectral statistics, CSR, and Ginibre ensemble behavior. This conclusion is supported by extensive analyses of the non-Hermitian Sachdev-Ye-Kitaev (SYK) model [31–38] and non-Hermitian random matrix ensembles [19, 26]. Together, these results establish the universality of KC as a diagnostic tool beyond the Hermitian realm and underscore its applicability to dissipative many-body systems.

Bi-lanczos algorithm. To investigate Krylov complexity in non-Hermitian many-body systems, we use the bi-Lanczos algorithm [39–41], an extension of the standard Lanczos procedure [42, 43] that accommodates the absence of a orthonormal basis.

The bi-Lanczos algorithm generates two sets of orthonormal Krylov bases, $\{|p_n\rangle\}$ and $\{|q_n\rangle\}$, subject to the bi-orthonormal condition $\langle p_n | q_m \rangle = \delta_{nm}$. Moreover, this procedure produces three sequences of Lanczos coefficients, $\{a_n, b_n, c_n\}$, that encode the dynamics of the system. These coefficients appear in the three-term recurrence relations of the bi-Lanczos algorithm for a given non-Hermitian Hamiltonian H :

$$\begin{aligned} |r_{n+1}\rangle &= (H - a_n)|q_n\rangle - b_n|q_{n-1}\rangle, & |q_n\rangle &= c_n^{-1}|r_n\rangle, \\ |l_{n+1}\rangle &= (H^\dagger - a_n^*)|p_n\rangle - c_n^*|p_{n-1}\rangle, & |p_n\rangle &= b_n^{*-1}|l_n\rangle, \end{aligned} \quad (1)$$

which iteratively generate the biorthogonal Krylov subspaces. In this basis, the non-Hermitian H admits a tridiagonal representation, in which the Lanczos coefficients directly correspond to its matrix elements:

$$T = \begin{pmatrix} a_0 & b_1 & 0 & \cdots & 0 \\ c_1 & a_1 & b_2 & \ddots & \vdots \\ 0 & c_2 & a_2 & \ddots & 0 \\ \vdots & \ddots & \ddots & \ddots & b_{n-1} \\ 0 & \cdots & 0 & c_{n-1} & a_{n-1} \end{pmatrix}, \quad (2)$$

where the a_n correspond to the main diagonal, the b_n to the superdiagonal, and the c_n to the subdiagonal elements. This tridiagonal form serves as the starting point for analyzing time evolution and computing Krylov complexity in non-Hermitian systems.

To compute KC, we first select two normalized initial states to seed the biorthogonal Krylov construction. In the Hermitian case, several studies have shown that the Krylov complexity computed from the thermofield double (TFD) state at infinite temperature, i.e., a maximally entangled state, exhibits a pronounced early-time peak, serving as an effective diagnostic of quantum chaos [2, 7, 9, 10]. Motivated by these observations, we adopt the normalized TFD state from [2] as the initial state in our non-Hermitian setup to test whether the same characteristic peak structure, and hence the conjectured diagnostic, persists. More precisely, we take:

$$|p_0\rangle = |q_0\rangle = |\text{TFD}\rangle, \quad (3)$$

as the initial state that seeds the bi-Lanczos algorithm, Eq. (1). Starting from this state, repeated applications of the Hamiltonian combined with the two-sided Gram-Schmidt procedure generate two sets of Krylov bases and the corresponding Lanczos coefficients.

The precise algorithm can be summarized as follows:

(i) Set: $b_0 = c_0 = 0$, $a_0 = \langle p_0 | H | q_0 \rangle = \langle q_0 | H | p_0 \rangle$;

(ii) For $n \geq 1$, define :

$$\begin{aligned} |r_n\rangle &= (H - a_{n-1})|q_{n-1}\rangle - b_{n-1}|q_{n-2}\rangle, \\ |l_n\rangle &= (H^\dagger - a_{n-1}^*)|p_{n-1}\rangle - c_{n-1}^*|p_{n-2}\rangle; \end{aligned}$$

- (iii) Compute: $c_n = \sqrt{|\langle r_n | l_n \rangle|}$, $b_n = c_n^{-1}\langle r_n | l_n \rangle$;
- (iv) Compute: $|q_n\rangle = c_n^{-1}|r_n\rangle$, $|p_n\rangle = b_n^{*-1}|l_n\rangle$;
- (v) Replace:
 - $|q_n\rangle \rightarrow |q_n\rangle - \sum_{l=1}^{n-1} \langle p_l | q_l \rangle |q_l\rangle$,
 - $|p_n\rangle \rightarrow |p_n\rangle - \sum_{l=1}^{n-1} \langle q_l | p_l \rangle |p_l\rangle$;
- (vi) Compute: $a_n = \langle p_n | H | q_n \rangle$;
- (vii) If $b_n = 0$ stop; otherwise go to step (ii).

In practice, numerical instabilities may arise due to the loss of full bi-orthogonality. To prevent the accumulation of such errors, it is necessary to perform complete bi-orthogonalization twice using the Gram-Schmidt procedure (v), which ensures that the generated Krylov basis vectors remain stable at every step. For further details on the numerical validation of our bi-Lanczos algorithm, we refer the reader to the Supplementary Material (SM).

Using either of the obtained Krylov bases, $|p_n\rangle$ or $|q_n\rangle$, any time-evolved state $|\Psi(t)\rangle$ can be expressed as

$$|\Psi(t)\rangle = \sum_{n=0} \Phi_n^p(t)|p_n\rangle = \sum_{n=0} \Phi_n^q(t)|q_n\rangle, \quad (4)$$

with coefficients $\Phi_n^p(t)$ and $\Phi_n^q(t)$, which define Krylov complexity in the non-Hermitian setting as

$$C(t) \equiv \sum_n n |\tilde{\Phi}_n^{p*}(t) \tilde{\Phi}_n^q(t)|. \quad (5)$$

Here, the tildes denote the dynamically normalized biorthogonal bases, which ensure that the Krylov probability remains conserved [44],

$$P(t) = \sum_n |\tilde{\Phi}_n^{p*}(t) \tilde{\Phi}_n^q(t)| = 1. \quad (6)$$

In prototypical Hermitian systems, e.g., random matrices [2, 3, 45–47], quantum billiards [48–50], and variants of the SYK model [7, 10, 11, 51], KC typically follows a characteristic dynamical pattern: an initial growth phase, a pronounced peak, and eventual saturation, with the peak often serving as a hallmark of quantum chaos.

In contrast, KC in non-Hermitian systems has been far less explored, leaving open the question of whether the characteristic peak persists as a universal chaos diagnostic. Progress is hindered by technical challenges: the bi-Lanczos algorithm requires the simultaneous construction of left and right Krylov bases, which are not mutually orthogonal. This doubles memory demands and amplifies numerical instabilities, often necessitating costly re-biorthogonalization. To mitigate these issues, some works restrict to complex-symmetric Hamiltonians and apply the standard Lanczos algorithm [44, 52, 53], while others retain the full bi-Lanczos approach [54] but limit themselves to smaller Hilbert spaces. Moreover, these studies have largely focused on phenomena such as the quantum Zeno effect, non-Hermitian phase transitions, or quantum Fisher information, rather than quantum chaos.

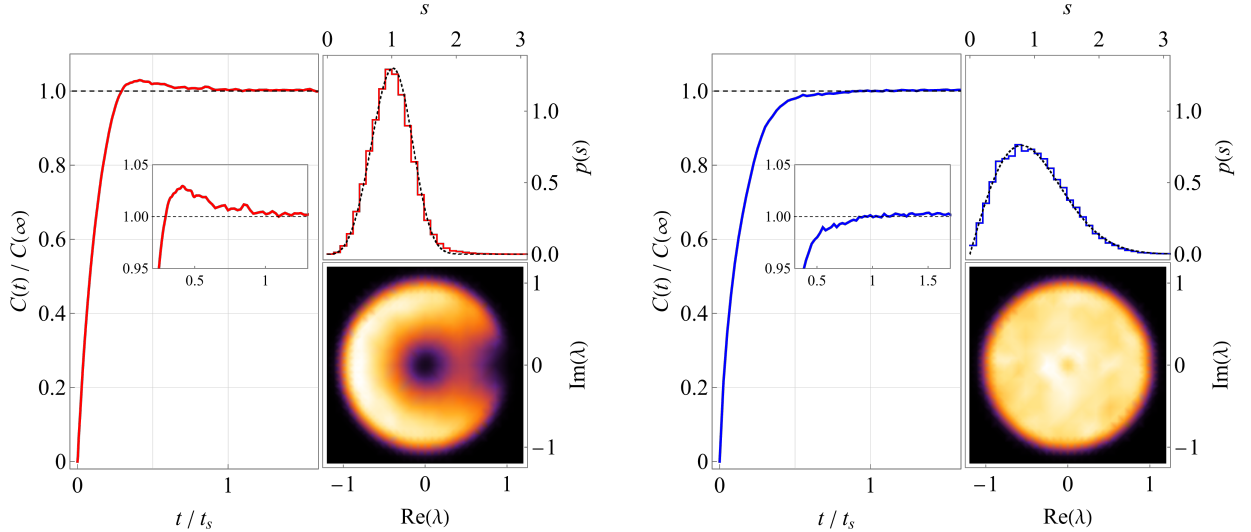


Figure 1. Unifying probes to diagnose quantum chaos in the non-Hermitian SYK model: Krylov complexity $C(t)$, complex level spacing distribution $p(s)$, and CSR in the complex plane. **Left:** For $q = 4$, clear signatures of quantum chaos are observed, including a pronounced peak in the Krylov complexity, agreement with GinUE statistics in the complex level spacing distribution, and anisotropic CSR. **Right:** In contrast, the $q = 2$ case shows no peak in Krylov complexity, a complex level spacing distribution consistent with two-dimensional Poisson statistics, and isotropic CSR.

A recent exception is Ref. [55], which examined a disordered non-Hermitian spin chain with the bi-Lanczos algorithm and conjectured that a suppression in the KC growth may signal chaotic-integrable transitions. Yet no peak was observed in either regime, likely due to the choice of the initial state that was not set to the TFD state. For related investigations of operator KC in open settings, see also [56–61].

Non-Hermitian SYK model. Our first application is the non-Hermitian SYK (nHSYK) model [36, 37], describing N Majorana fermions in $(0+1)$ dimensions with random q -body interactions. It extends the original SYK model [62–64] by including an additional non-Hermitian term. Its Hamiltonian is given by

$$H = \sum_{i_1 < i_2 < \dots < i_q}^N (J_{i_1 i_2 \dots i_q} + i M_{i_1 i_2 \dots i_q}) \chi_{i_1} \chi_{i_2} \dots \chi_{i_q}, \quad (7)$$

where χ_i are Majorana fermions satisfying $\{\chi_i, \chi_j\} = \delta_{ij}$. The random couplings J and M are drawn from Gaussian distributions with zero mean and variance $\langle J^2 \rangle = \langle M^2 \rangle = (q-1)!/N^{q-1}$. A nonzero M explicitly breaks the system's Hermiticity. In our simulations, we take $N = 22$ for both $q = 4$ and $q = 2$, incorporating a parity-symmetry block to reduce the effective dimension.

To benchmark our results, we analyze the KC alongside the complex level spacing distribution and CSR in the non-Hermitian SYK model, where CSR is defined [19] by

$$\lambda_k = \frac{E_k^{\text{NN}} - E_k}{E_k^{\text{NNNN}} - E_k}, \quad (8)$$

with E_k denoting a complex eigenvalue and E_k^{NN} , E_k^{NNNN} its nearest and next-to-nearest neighbors. Observables

are averaged over 1000 independent realizations to ensure convergence and reduce numerical error. Our results are shown in Fig. 1. For convenience, KC is rescaled so that its late-time saturation value $C(\infty)$ equals unity, with the saturation time t_s defined accordingly.

The left panel of Fig. 1 displays clear signatures of quantum chaos for $q = 4$, consistently observed across all three diagnostics. The KC, computed exactly using the bi-Lanczos algorithm, exhibits a distinct peak consistent with the spectral statistics of non-Hermitian random matrix theory. The complex eigenvalue spacing distribution $p(s)$ closely follows that of complex Gaussian non-Hermitian random matrices (GinUE) [14],

$$p(s) = \left(\prod_{k=1}^{\infty} \frac{\Gamma(1+k, s^2)}{k!} \right) \sum_{j=1}^{\infty} \frac{2s^{2j+1} e^{-s^2}}{\Gamma(1+j, s^2)}, \quad (9)$$

where $\Gamma(1+k, s^2) = \int_{s^2}^{\infty} t^k e^{-t} dt$ is the incomplete gamma function. Finally, the CSR displays strong suppression at small angles, with anisotropy in the angular distribution quantified by $\langle \cos \theta \rangle \approx 0.22$, close to the GinUE value [19].

In contrast, the right panel of Fig. 1 ($q = 2$) shows clear signatures of integrability: no peak in KC, a complex eigenvalue spacing distribution following the two-dimensional Poisson distribution [14], and a nearly isotropic CSR, with $\langle \cos \theta \rangle \approx 0.003$ for $\theta = [0, 2\pi]$.

In non-Hermitian settings, the Lanczos coefficients are found to satisfy a universal relation absent in Hermitian systems: $(1/\sqrt{2})|a_n| \approx |b_n| = c_n$, with the second equality holding by construction of the bi-Lanczos algorithm. In contrast, a_n are weakly structured in standard closed systems [2]. Fig. 2 shows the Lanczos coefficients of the nHSYK model with $q = 4$ (red) and $q = 2$ (blue), demon-

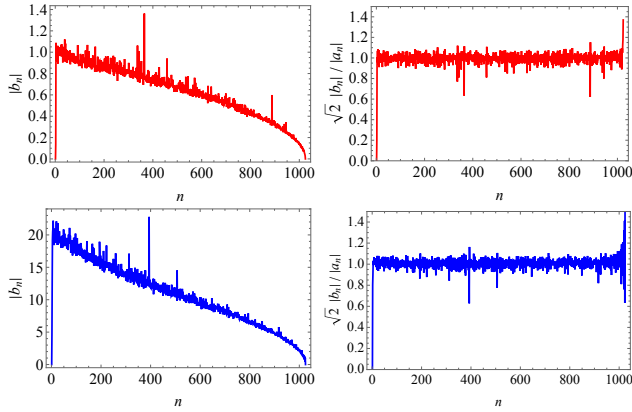


Figure 2. Lanczos coefficients for the nHSYK model. **Top:** chaotic case ($q = 4$); **Bottom:** integrable case ($q = 2$). Unlike the Hermitian setting, the magnitudes of the complex Lanczos coefficients are found to satisfy $(1/\sqrt{2})|a_n| \approx |b_n| = c_n$.

strating that this relation persists in the non-Hermitian setting, regardless of whether the system is chaotic or integrable. This proportionality reflects a balanced tight-binding Krylov chain with fixed ratios between onsite and hopping amplitudes (see Supplementary Material).

Non-Hermitian random matrix universality. In Hermitian random matrices, Dyson’s classification into three symmetry classes (A, AI, AII) yields distinct universal behaviors characterized by Gaussian Orthogonal (GOE), Gaussian Unitary (GUE), or Gaussian Symplectic (GSE) statistics. In the non-Hermitian case, Ginibre used the same symmetry labels, all of which were found to correspond to a single universal type, the GinUE [16] (class A). More recently, it has been shown that even in the non-Hermitian setting, three distinct universal behaviors, corresponding to classes A, AI^\dagger , and AII^\dagger , can be identified by considering an alternative symmetry involving transposition and complex conjugation [26].

It is worth noting that all symmetry classes of non-Hermitian random matrices can be explored using the $q = 4$ nHSYK model by varying the number of Majorana fermions [21]; for example, $N = 22$ yields results consistent with class A. As a second application, and to test the universality of our findings, we focus directly on non-Hermitian random matrix theories. To remain within the same symmetry class throughout this work, we choose the class A model. For comparison, and to illustrate two-dimensional Poisson statistics, we also consider a non-Hermitian random matrix with completely uncorrelated eigenvalues, which is expected to yield results consistent with the $q = 2$ integrable nHSYK model.

Our findings from the non-Hermitian random matrix model under consideration closely match those from the nHSYK model, reinforcing the correspondence between them (Fig. 3). This suggests that key features of the nHSYK model, including those revealed by the bi-Lanczos algorithm, may be universal in non-Hermitian

systems with random matrix behavior. In the chaotic phase: (i) a distinct KC peak, (ii) complex spacing statistics consistent with GinUE, and (iii) anisotropic CSR are observed. In the integrable phase: (i) no KC peak, (ii) two-dimensional Poisson spacing statistics, and (iii) isotropic CSR are found. Furthermore, the Lanczos-coefficient relation $(1/\sqrt{2})|a_n| \approx |b_n| = c_n$ holds in random matrix models as well.

Discussion. In this work, we have shown that Krylov complexity (KC), defined through the bi-Lanczos algorithm, serves as a robust and universal probe of quantum chaos in non-Hermitian systems. The early-time KC peak, recognized as a hallmark of chaos in Hermitian systems, persists in open settings, in agreement with complex spectral diagnostics such as Ginibre statistics (GinUE) and anisotropic complex spacing ratios (CSR).

Through detailed analyses of the non-Hermitian SYK model and random matrix ensembles, we identify model-independent indicators of chaos, revealing universal behaviors across systems within the same symmetry class. Specifically, in chaotic regimes, we find a clear KC peak, GinUE-level spacing, and anisotropic CSR; in integrable regimes, these are replaced by the absence of a KC peak, two-dimensional Poisson statistics, and isotropic CSR. These results reinforce the universality of KC as a diagnostic of quantum chaos and underscore the effectiveness of biorthogonal Krylov dynamics in capturing spectral correlations and information spreading.

Looking ahead, it will be valuable to extend this framework to other non-Hermitian symmetry classes (AI^\dagger and AII^\dagger) and to systematically explore its scaling with system size and degree of non-Hermiticity. Equally promising is the search for connections with dynamical probes accessible in experimental platforms that emulate non-Hermitian Hamiltonians. In addition, generalizing other Krylov-space tools from closed systems, such as Krylov entropy [65], which quantifies the randomness of the probability distribution, and the Krylov metric [66], which tracks the geometric growth of the Krylov subspace, could uncover new signatures of chaos in open quantum systems. Altogether, these directions promise to establish the bi-Lanczos Krylov dynamics as a robust, unifying framework for diagnosing quantum chaos across the full landscape of non-Hermitian many-body systems.

Acknowledgements. MB and KBH acknowledge the support of the Foreign Young Scholars Research Fund Project (Grant No.22Z033100604). MB acknowledges the sponsorship from the Yangyang Development Fund. HSJ and JFP are supported by the Spanish MINECO ‘Centro de Excelencia Severo Ochoa’ program under grant SEV-2012-0249, the Comunidad de Madrid ‘Atracción de Talento’ program (ATCAM) grant 2020-T1/TIC-20495, the Spanish Research Agency via grants CEX2020-001007-S and PID2021-123017NB-I00, funded by MCIN/AEI/10.13039/501100011033, and ERDF ‘A way of making Europe.’ KYK was supported by the Basic Science Research Program through the National

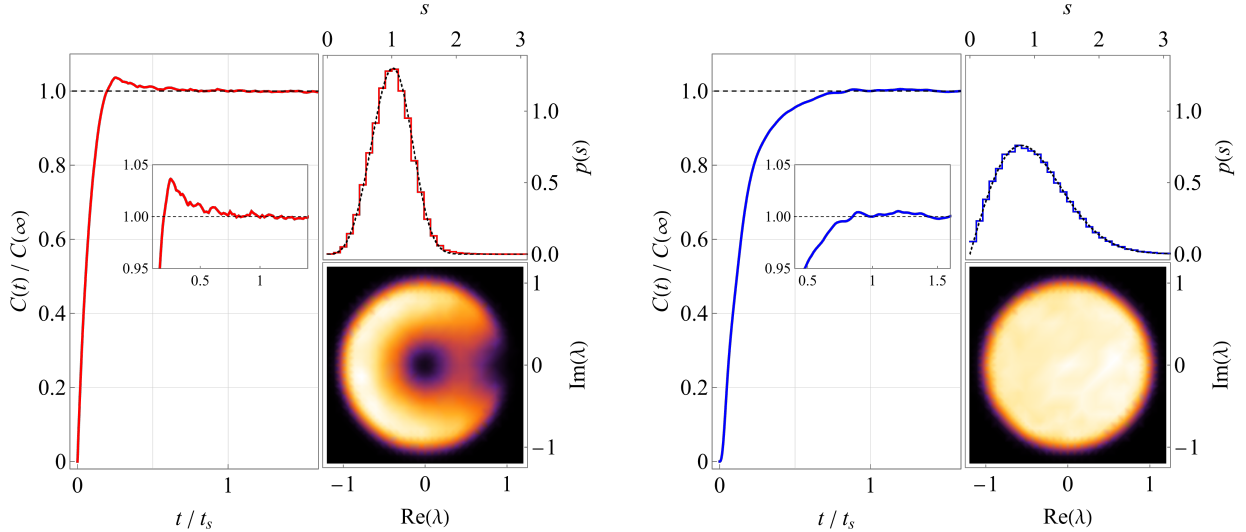


Figure 3. Unifying probes to diagnose quantum chaos in the non-Hermitian random matrix model: Krylov complexity $C(t)$, complex level spacing distribution $p(s)$, and CSR in the complex plane. **Left:** For a class A random matrix, distinct signatures of quantum chaos are observed, including a pronounced KC peak, agreement with GinUE statistics in the complex level spacing distribution, and anisotropic CSR. **Right:** In contrast, the uncorrelated diagonal random matrix shows no KC peak, a complex level spacing distribution consistent with two-dimensional Poisson statistics, and isotropic CSR.

Research Foundation of Korea (NRF) funded by the Ministry of Science, ICT & Future Planning (NRF-2021R1A2C1006791) and the AI-based GIST Research Scientist Project grant funded by the GIST in 2025. KYK was also supported by the Creation of the Quantum Information Science R&D Ecosystem (Grant No. 2022M3H3A106307411) through the National Research

Foundation of Korea (NRF) funded by the Korean government (Ministry of Science and ICT). HSJ would like to thank the Asia Pacific Center for Theoretical Physics (APCTP) for their hospitality during the program *Holography 2025: Quantum Matter and Entanglement*, where parts of this work were undertaken.

-
- [1] D. E. Parker, X. Cao, A. Avdoshkin, T. Scaffidi, and E. Altman, *Phys. Rev. X* **9**, 041017 (2019), [arXiv:1812.08657 \[cond-mat.stat-mech\]](#).
- [2] V. Balasubramanian, P. Caputa, J. M. Magan, and Q. Wu, *Phys. Rev. D* **106**, 046007 (2022), [arXiv:2202.06957 \[hep-th\]](#).
- [3] P. Caputa, H.-S. Jeong, S. Liu, J. F. Pedraza, and L.-C. Qu, *JHEP* **05**, 337 (2024), [arXiv:2402.09522 \[hep-th\]](#).
- [4] P. Nandy, A. S. Matsoukas-Roubeas, P. Martínez-Azcona, A. Dymarsky, and A. del Campo, *Phys. Rept.* **1125-1128**, 1 (2025), [arXiv:2405.09628 \[quant-ph\]](#).
- [5] E. Rabinovici, A. Sánchez-Garrido, R. Shir, and J. Sonner, (2025), [arXiv:2507.06286 \[hep-th\]](#).
- [6] P. Caputa and S. Datta, *JHEP* **12**, 188 (2021), [Erratum: *JHEP* 09, 113 (2022)], [arXiv:2110.10519 \[hep-th\]](#).
- [7] J. Erdmenger, S.-K. Jian, and Z.-Y. Xian, *JHEP* **08**, 176 (2023), [arXiv:2303.12151 \[hep-th\]](#).
- [8] G. F. Scialchi, A. J. Roncaglia, and D. A. Wisnacki, *Phys. Rev. E* **109**, 054209 (2024), [arXiv:2309.13427 \[quant-ph\]](#).
- [9] H. A. Camargo, K.-B. Huh, V. Jahnke, H.-S. Jeong, K.-Y. Kim, and M. Nishida, *JHEP* **08**, 241 (2024), [arXiv:2405.11254 \[hep-th\]](#).
- [10] M. Baggio, K.-B. Huh, H.-S. Jeong, K.-Y. Kim, and J. F. Pedraza, *Phys. Rev. Res.* **7**, 023028 (2025), [arXiv:2407.17054 \[hep-th\]](#).
- [11] K.-B. Huh, H.-S. Jeong, L. A. Pando Zayas, and J. F. Pedraza, *Phys. Rev. D* **111**, L121902 (2025), [arXiv:2412.04963 \[hep-th\]](#).
- [12] Y. Ashida, Z. Gong, and M. Ueda, *Adv. Phys.* **69**, 249 (2021), [arXiv:2006.01837 \[cond-mat.mes-hall\]](#).
- [13] A. Rivas and S. F. Huelga, *Open Quantum Systems: An Introduction* (Springer Berlin Heidelberg, 2012).
- [14] R. Grobe, F. Haake, and H.-J. Sommers, *Phys. Rev. Lett.* **61**, 1899 (1988).
- [15] R. Grobe, *Physical Review Letters* **62**, 2893 (1989).
- [16] J. Ginibre, *J. Math. Phys.* **6**, 440 (1965).
- [17] R. Hamazaki, K. Kawabata, and M. Ueda, (2018), [10.1103/PhysRevLett.123.090603, 1811.11319](#).
- [18] G. Akemann, M. Kieburg, A. Mielke, and T. Prosen, *Phys. Rev. Lett.* **123**, 254101 (2019), [1910.03520](#).
- [19] L. Sá, P. Ribeiro, and T. Prosen, *Phys. Rev. X* **10**, 021019 (2020), [1910.12784](#).
- [20] J. Li, T. Prosen, and A. Chan, (2021), [2110.03444](https://doi.org/10.1103/PhysRevLett.127.170602, 2103.05001.</p>
<p>[21] A. M. García-García, L. Sá, and J. J. M. Verbaarschot, <i>Phys. Rev. X</i> 12, 021040 (2022), <a href=).

- [22] S. Shivam, A. D. Luca, D. A. Huse, and A. Chan, *Phys. Rev. Lett.* **130**, 140403 (2023), arXiv:2207.12390.
- [23] M. V. Berry and M. Tabor, *Proceedings of the Royal Society of London. Series A, Mathematical and Physical Sciences* **356**, 375 (1977).
- [24] O. Bohigas, M. J. Giannoni, and C. Schmit, *Phys. Rev. Lett.* **52**, 1 (1984).
- [25] M. L. Mehta, *Random Matrices*, 3rd ed. (2004).
- [26] R. Hamazaki, K. Kawabata, N. Kura, and M. Ueda, *Phys. Rev. Res.* **2**, 023286 (2020).
- [27] Y. Y. Atas, *Physical Review Letters* **110** (2013), 10.1103/PhysRevLett.110.084101.
- [28] K. Kawabata, Z. Xiao, T. Ohtsuki, and R. Shindou, *PRX Quantum* **4**, 040312 (2023), arXiv:2307.08218 [cond-mat.mes-hall].
- [29] P. Nandy, T. Pathak, Z.-Y. Xian, and J. Erdmenger, (2024), arXiv:2411.09309 [quant-ph].
- [30] M. Baggiooli, K.-B. Huh, H.-S. Jeong, X. Jiang, K.-Y. Kim, and J. F. Pedraza, *Phys. Rev. D* **111**, L101904 (2025), arXiv:2503.11274 [hep-th].
- [31] A. M. García-García and V. Godet, *Phys. Rev. D* **103**, 046014 (2021), arXiv:2010.11633 [hep-th].
- [32] K. Su, P. Zhang, and H. Zhai, *JHEP* **21**, 156 (2020), arXiv:2101.11238 [cond-mat.str-el].
- [33] C. Liu, P. Zhang, and X. Chen, *SciPost Phys.* **10**, 048 (2021), arXiv:2008.11955 [cond-mat.str-el].
- [34] A. M. García-García, Y. Jia, D. Rosa, and J. J. M. Verbaarschot, *Phys. Rev. Lett.* **128**, 081601 (2022), arXiv:2102.06630 [hep-th].
- [35] P. Zhang, S.-K. Jian, C. Liu, and X. Chen, *Quantum* **5**, 579 (2021), arXiv:2104.04088 [cond-mat.str-el].
- [36] A. M. García-García, L. Sá, and J. J. M. Verbaarschot, *Phys. Rev. X* **12**, 021040 (2022), arXiv:2110.03444 [hep-th].
- [37] A. M. García-García, Y. Jia, D. Rosa, and J. J. M. Verbaarschot, *Phys. Rev. D* **105**, 126027 (2022), arXiv:2203.13080 [hep-th].
- [38] G. Cipolloni and J. Kudler-Flam, *Phys. Rev. Lett.* **130**, 010401 (2023), arXiv:2206.12438 [cond-mat.stat-mech].
- [39] S. W. Gaaf and E. Jarlebring, *SIAM Journal on Scientific Computing* **39**, S898 (2017).
- [40] *Templates for the Solution of Algebraic Eigenvalue Problems: A Practical Guide* (Society for Industrial and Applied Mathematics, 2000).
- [41] M. Grüning, A. Marini, and X. Gonze, (2011), 1102.3909.
- [42] C. Lanczos, *J. Res. Natl. Bur. Stand. B* **45**, 255 (1950).
- [43] V. S. Viswanath and G. Müller, *The Recursion Method: Application to Many-Body Dynamics* (Springer Berlin, Heidelberg, Germany, 1994).
- [44] A. Bhattacharya, R. N. Das, B. Dey, and J. Erdmenger, *JHEP* **03**, 179 (2024), arXiv:2312.11635 [hep-th].
- [45] V. Balasubramanian, J. M. Magan, and Q. Wu, (2023), arXiv:2312.03848 [hep-th].
- [46] B. Bhattacharjee and P. Nandy, *Phys. Rev. B* **111**, L060202 (2025), arXiv:2407.07399 [quant-ph].
- [47] H.-S. Jeong, A. Kundu, and J. F. Pedraza, *JHEP* **05**, 154 (2025), arXiv:2412.12301 [hep-th].
- [48] K. Hashimoto, K. Murata, N. Tanahashi, and R. Watanabe, *JHEP* **11**, 040 (2023), arXiv:2305.16669 [hep-th].
- [49] K.-B. Huh, H.-S. Jeong, and J. F. Pedraza, *JHEP* **05**, 137 (2024), arXiv:2312.12593 [hep-th].
- [50] V. Balasubramanian, R. N. Das, J. Erdmenger, and Z.-Y. Xian, *J. Stat. Mech.* **2025**, 033202 (2025), arXiv:2407.11114 [hep-th].
- [51] S. Chapman, S. Demulder, D. A. Galante, S. U. Sheorey, and O. Shoval, *Phys. Rev. B* **111**, 035141 (2025), arXiv:2407.09604 [hep-th].
- [52] E. Medina-Guerra, I. V. Gornyi, and Y. Gefen, *Phys. Rev. B* **111**, 174207 (2025), arXiv:2502.07775 [quant-ph].
- [53] E. Medina-Guerra, I. V. Gornyi, and Y. Gefen, *Phys. Rev. B* **112**, 035427 (2025), arXiv:2503.18936 [cond-mat.str-el].
- [54] N. Chakrabarti, N. Nirbhan, and A. Bhattacharyya, *JHEP* **07**, 203 (2025), arXiv:2502.03434 [quant-ph].
- [55] Y. Zhou, W. Xia, L. Li, and W. Li, (2025), arXiv:2501.15982 [quant-ph].
- [56] C. Liu, H. Tang, and H. Zhai, *Phys. Rev. Res.* **5**, 033085 (2023), arXiv:2207.13603 [cond-mat.str-el].
- [57] A. Bhattacharya, P. Nandy, P. P. Nath, and H. Sahu, *JHEP* **12**, 081 (2022), arXiv:2207.05347 [quant-ph].
- [58] N. S. Srivatsa and C. von Keyserlingk, *Physical Review B* **109** (2024), 10.1103/physrevb.109.125149.
- [59] B. Bhattacharjee, X. Cao, P. Nandy, and T. Pathak, *JHEP* **03**, 054 (2023), arXiv:2212.06180 [quant-ph].
- [60] A. Bhattacharya, P. Nandy, P. P. Nath, and H. Sahu, *JHEP* **12**, 066 (2023), arXiv:2303.04175 [quant-ph].
- [61] A. Bhattacharyya, S. S. Haque, G. Jafari, J. Murugan, and D. Rapotu, *JHEP* **10**, 157 (2023), arXiv:2307.15495 [hep-th].
- [62] S. Sachdev and J. Ye, *Phys. Rev. Lett.* **70**, 3339 (1993).
- [63] S. Sachdev, *Phys. Rev. X* **5**, 041025 (2015).
- [64] J. Maldacena and D. Stanford, *Phys. Rev. D* **94**, 106002 (2016).
- [65] J. L. F. Barbón, E. Rabinovici, R. Shir, and R. Sinha, *JHEP* **10**, 264 (2019), arXiv:1907.05393 [hep-th].
- [66] L. Chen, B. Mu, H. Wang, and P. Zhang, *Phys. Rev. Lett.* **134**, 190403 (2025), arXiv:2404.08207 [quant-ph].

SUPPLEMENTARY MATERIAL

This Supplementary Material presents additional details on the numerical computations with bi-Lanczos algorithm discussed in the main text and present further analyses to corroborate our findings.

A. Krylov Chain Interpretation of Non-Hermitian Lanczos Coefficients

In the Hermitian Lanczos algorithm, a single orthonormal basis $\{|q_n\rangle\}$ is generated by a three-term recursion. This yields a tridiagonal representation of the Hamiltonian with coefficients

$$a_n = \langle q_n | H | q_n \rangle, \quad b_{n+1} = \langle q_n | H | q_{n+1} \rangle = c_{n+1}, \quad (10)$$

such that the resulting tridiagonal matrix (2) is symmetric.

On the other hand, in the non-Hermitian case, a single Krylov basis is no longer sufficient to span the whole space or lose the tridiagonal structure, since the eigenvectors of H and H^\dagger from two distinct families. The bi-Lanczos procedure therefore constructs two bi-orthogonal bases,

$$\{|q_n\rangle\}, \quad \{\langle p_n |\}, \quad (11)$$

constrained by the bi-orthogonality condition $\langle p_n | q_m \rangle = \delta_{nm}$. This two-ladder construction preserves the tridiagonal form of the reduced Hamiltonian while maintaining stability of the recursion.

The associated bi-Lanczos coefficients are defined by

$$a_n = \langle p_n | H | q_n \rangle, \quad b_{n+1} = \langle p_n | H | q_{n+1} \rangle, \quad c_{n+1} = \langle p_{n+1} | H | q_n \rangle, \quad (12)$$

together with their conjugates obtained from H^\dagger . These coefficients govern the “hopping” dynamics of the Krylov chains: (a_n acts as an onsite term, while b_n and c_n describe nearest-neighbor transitions):

$$H | q_n \rangle = a_n | q_n \rangle + b_n | q_{n-1} \rangle + c_{n+1} | q_{n+1} \rangle, \quad H^\dagger | p_n \rangle = a_n^* | p_n \rangle + c_n^* | p_{n-1} \rangle + b_{n+1}^* | p_{n+1} \rangle, \quad (13)$$

obtained from the recursion relation of Eq. (1). Each chain looks like a 1D hopping chain, but we need both chains simultaneously to represent a non-Hermitian H . In other words, the chains are “coupled” in the sense that all coefficients are defined as overlaps $\langle p_n | H | q_m \rangle$. This means the hopping strength on the q -chain is controlled by how the q -chain and p -chain pair up: See Fig. 4 for a schematic illustration of the coupled Krylov chains.

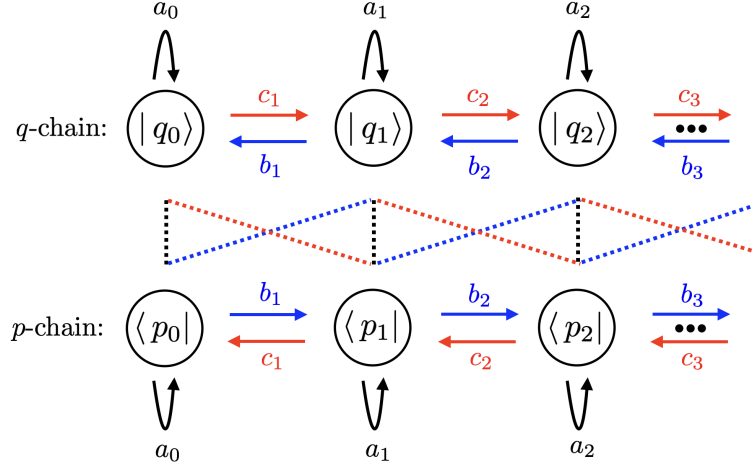


Figure 4. Schematic representation of the Hamiltonian action on the Krylov chains, Eq. (13). Each site carries an on-site term a_n (self-loop), while b_n and c_n denote left and right hopping amplitudes. The dashed lines indicate the overlaps $\langle p_n | H | q_m \rangle$, which determine the coefficients (a_n, b_n, c_n) in Eq. (12).

Empirical Observation. In extensive numerical experiments with large- N non-Hermitian models (including SYK-type systems and random matrix ensembles), we consistently observed the approximate relation

$$\frac{1}{\sqrt{2}} |a_n| \approx |b_n| = c_n. \quad (14)$$

This proportionality appeared robust across both chaotic and integrable cases, pointing to a universal geometric mechanism rather than model-specific details. It suggests that many seemingly different non-Hermitian Hamiltonians reduce to the same effective recursion: a balanced tight-binding ladder with fixed ratios between onsite and hopping amplitudes.

The origin of this universality may be traced to the structure of the bi-Lanczos recursion. Unlike the Hermitian algorithm, where a_n and b_n emerge from independent orthogonalization steps, the bi-Lanczos scheme enforces the strong constraint of bi-orthogonality, $\langle p_n | q_m \rangle = \delta_{nm}$. This condition can constrain how the action of H distributes over the amplitudes among a_n , b_n , and c_n , forcing them to share a common “normalization budget” to keep the bi-orthogonality condition in the balanced way.

Heuristically, one can view this as a Pythagorean-type constraint: the onsite weight a_n and the hopping terms b_n, c_n must balance in order to preserve bi-orthogonality. This coupling naturally drives the coefficients toward the approximate relation Eq. (14).

In chaotic matrix models, the relation may sharp in the large- N limit due to self-averaging, which suppresses fluctuations in the recursion coefficients. In contrast, in integrable systems the same proportionality still emerges numerically, but its robustness there appears to stem from geometric constraints of the bi-orthogonal Lanczos construction rather than statistical averaging. A systematic analytic distinction between these cases remains an open question.

We emphasize that this explanation is heuristic. While our observations strongly support the existence of a universal $\sqrt{2}$ proportionality, a complete analytic derivation is still lacking. Establishing a rigorous proof would not only validate this conjecture but also provide new insights into the geometric structure of effective non-Hermitian Krylov dynamics. We believe such an analysis is both feasible and worthwhile for future work.

B. Numerical Implementation and Validation

To establish the reliability of the bi-Lanczos algorithm, we perform a systematic numerical validation to ensure that the results used in our analysis of Krylov complexity for non-Hermitian models are trustworthy. The algorithm generates two main outputs: (I) two sets of Krylov bases, and (II) the associated Lanczos coefficients. The validation proceeds in two stages, each addressing one of these outputs.

(I) Bi-orthonormality of the Krylov bases. We first verify that the constructed bases satisfy the bi-orthonormal condition

$$\langle p_n | q_m \rangle = \delta_{nm} . \quad (15)$$

Numerical evaluation confirms this property: as shown in Fig. 5, all off-diagonal elements of the Gram matrix are suppressed to machine precision, while the diagonal entries remain equal to unity within numerical accuracy, i.e., at the order of $\mathcal{O}(10^{-16})$. This confirms that the bases produced by the bi-Lanczos procedure are indeed bi-orthonormal.

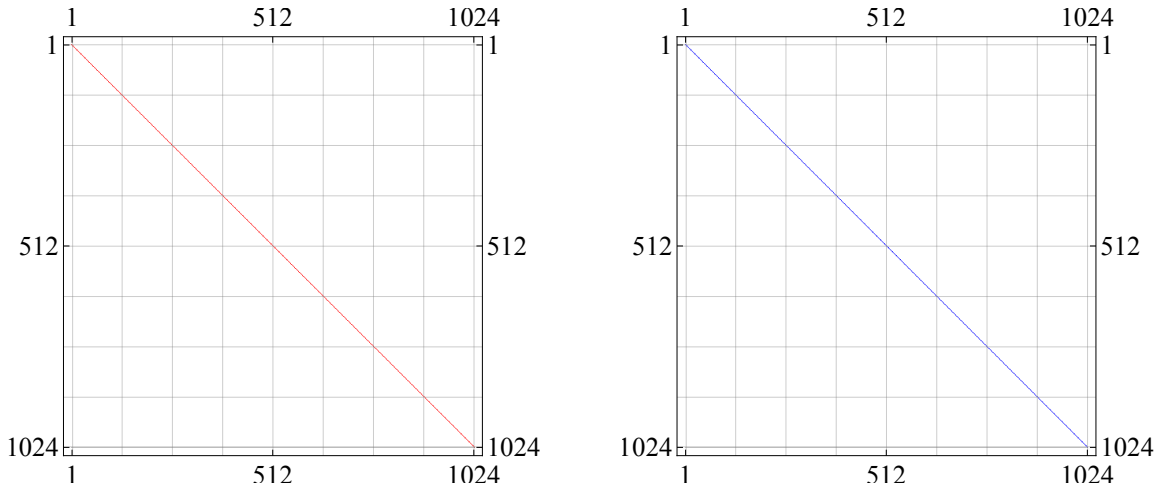


Figure 5. Verification of the bi-orthonormal condition $\langle q_n | p_m \rangle = \delta_{mn}$ for the non-Hermitian SYK model with $q = 4$ (left) and $q = 2$ (right).

(II) Accuracy of the Lanczos coefficients and tri-diagonalization. Next, we assess the correctness of the Lanczos coefficients by checking the tri-diagonalization they produce. From the numerically obtained coefficients, we construct the tri-diagonal matrix T , Eq. (2), and compute its eigenvalues E_n^T . These are then compared with the eigenvalues of the original Hamiltonian H , E_n^H . The difference,

$$\Delta E_n \equiv E_n^T - E_n^H, \quad (16)$$

quantifies the reliability of the procedure. Fig. 6 shows that $\Delta E_n \approx \mathcal{O}(10^{-16})$, confirming the precision of the tri-diagonalization.

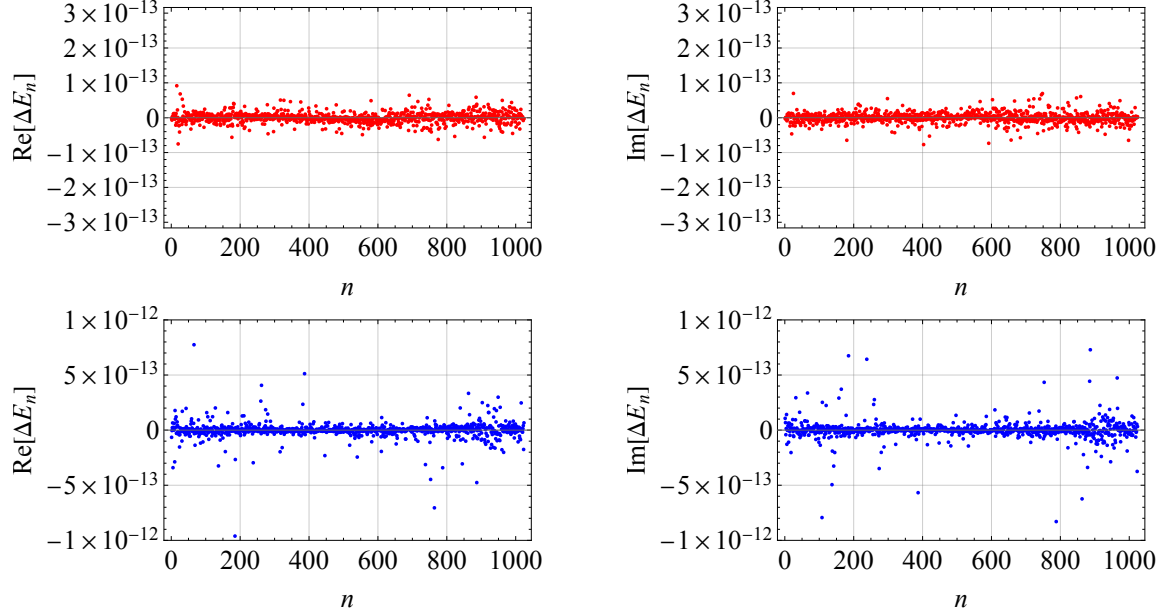


Figure 6. Comparison of the complex eigenvalue spectra ΔE_n for the non-Hermitian SYK model with $q = 4$ (top) and $q = 2$ (bottom).

We illustrated the validation of the bi-Lanczos algorithm for the non-Hermitian SYK models, but we repeated the same analysis for a non-Hermitian random matrix model and found consistent results, which are not shown here. Taken together, all these findings provide strong evidence for the robustness and numerical reliability of our implementations of the bi-Lanczos algorithm.